Journal of Power Sources 196 (2011) 7945–7950

Contents lists available at ScienceDirect

Journal of Power Sources

journal homepage: www.elsevier.com/locate/jpowsour

Highly active rhodium/carbon nanocatalysts for ethanol oxidation in alkaline medium

Yange Suo, I-Ming Hsing*

Department of Chemical and Biomolecular Engineering, The Hong Kong University of Science and Technology, Clear Water Bay, Kowloon, Hong Kong, China

ARTICLE INFO

Article history:
Received 13 January 2011
Received in revised form 17 May 2011
Accepted 19 May 2011
Available online 27 May 2011

Keywords:
Rhodium
Palladium
Ethanol oxidation
Alkaline

ABSTRACT

We report the synthesis and electrochemical characterization of rhodium/carbon (Rh/C) and palladium–rhodium/carbon (Pd–Rh/C) nanocatalysts for ethanol oxidation. Our results, for the first time, demonstrated that in an alkaline environment, Rh/C shows a much higher catalytic activity at low potential range than that of Pd–Rh/C and Pd/C. Intermediate species are produced during the oxidation process on Rh/C, as revealed by the complex impedance spectra (e.g., pseudo-inductive loop) at low potential range (i.e., −0.5 to −0.3 V). Adsorbed oxygen species, which are generated at high potentials, block active surface sites of Rh/C, resulting in the negative polarization resistance.

1. Introduction

Electro-oxidation reaction of ethanol is attracting an increasing amount of attention because of its application in direct ethanol fuel cells [1]. Several electrocatalytic materials have been reported for ethanol oxidation in an acidic medium [2]. In particular, the remarkable ternary Pt/Rh/SnO_2 electrocatalyst synthesized by Adzic's group has shown very high ethanol oxidizing efficiency [3]. However, in spite of the recent advancement, breaking C–C bond in ethanol in acidic solutions is still difficult. The efficiency of ethanol oxidation in alkaline solutions, on the other hand, has been demonstrated to be higher than that in the acidic counterpart [4]. Moreover, from the fuel cell standpoint, the development of new alkaline membrane [5] has created opportunities for alkaline direct ethanol fuel cells and stimulated research interests for electrocatalysts in alkaline medium [6]. Pd/C, which shows no activity for ethanol oxidation in acidic mediums [7], is reported to be more active than Pt/C in an alkaline environment for ethanol oxidation [8]. Pd-based binary (e.g., Pd–Au, Pd–Cu) catalysts have also been demonstrated to exhibit improved activity compared with pure Pd [9,10]. However, the difficulty of breaking C–C bond on Pd limits its catalytic activity and results in the production of acetate ions in concentrated alkaline solutions [11,12]. On the other hand, in a multimetallic catalyst setting, Rh contributes to the breakage of C–C bond on a Pt/Rh electrode and enhances the total oxidation of ethanol to CO_2 in an acidic environment [13], although Rh alone has very low electrochemical activity in an acidic solution.

In this work, we report the synthesis of Rh/C and Pd–Rh/C nanocatalysts for ethanol electro-oxidation in an alkaline solution. The carbon supported catalysts were synthesized using ethylene glycol and sodium acetate as the reducing and stabilizing reagents. Our electrochemical evaluation shows that Rh/C exhibits a much higher activity than Pd–Rh/C or Pd/C for ethanol oxidation in an alkaline medium. Distinct impedance behaviors of ethanol oxidation on Pd/C and Rh/C indicate a possibility of different reaction pathways on these two catalysts.

2. Experimental

2.1. Chemicals

Ammonium tetrachloropalladate ($(NH_4)_2PdCl_4$, 99.995%), rhodium chloride hydrate ($RhCl_3{\cdot}xH_2O$, 99.98%), ethylene glycol ($C_2H_6O_2$, 99.5%) were purchased from Sigma–Aldrich. Sodium citrate ($C_6H_5Na_3O_7{\cdot}2H_2O$, 99%), potassium hydroxide (KOH, 85%) and ethanol (C_2H_5OH, 99.5%) were ordered from BDH. Vulcan XC-72 carbon was purchased from E-TEK. Nafion solution (5%) was received from Dupont. Sulfuric acid (H_2SO_4, 95–98%) was purchased from Merck.

2.2. Synthesis of the catalysts

Pd/C, Rh/C and Pd–Rh/C (atomic ratio of Pd to Rh of 2:1) catalysts with 20 wt% metallic loadings were synthesized according to our previous report using ethylene glycol and sodium citrate

* Corresponding author. Tel.: +852 23587131; fax: +852 31064857.
E-mail address: kehsing@ust.hk (I-M. Hsing).

0378-7753/$ – see front matter © 2011 Elsevier B.V. All rights reserved.
doi:10.1016/j.jpowsour.2011.05.048

as the reducing and stabilizing reagents [14]. The preparation of Rh/C is described as an example to illustrate the synthesis procedures. Firstly, 18.6 mg sodium citrate was dissolved into 50 ml water/ethylene glycol mixture solution (volume/volume = 1:1), and then 26.1 mg Vulcan XC-72 carbon was poured into the above solution to obtain the sodium citrate suspension, which was stirred and ultrasonically mixed for 2 h. At the same time, 1.63 ml rhodium chloride hydrate ($RhCl_3{\cdot}xH_2O$) aqueous solution (1 g/100 ml) was mixed with another 10 ml water/ethylene glycol solution (volume/volume = 1:1) to obtain the precursor solution. After removing air with Ar gas bubbling for 30 min, the sodium citrate suspension was refluxed at 170 °C oil bath. After 5 min heating, the precursor solution was added into the heated sodium citrate suspension drop by drop. Another 40 ml water/ethylene glycol solution (volume/volume = 1:1) was added into the reaction system, which was continued to be heated for another 2 h. The reaction product was filtered and washed with water and ethanol. The residue was dried at 60 °C for 12 h and then grounded in an agate mortar.

2.3. Physicochemical characterization

Powder X-ray diffraction (XRD) was carried out with a powder diffraction system (Model PW 1830, Philips) using a Cu Kα radiation source operating at 40 kV and 40 mA. Transmission electron microscopy (TEM) was carried out with a JEOL 2010F TEM system operated with LaB6 filament at 200 kV. The samples were prepared by dropping catalyst suspensions (prepared by dispersing the catalysts ultrasonically in ethanol) onto carbon coated Cu grids and then dried at room temperature. Average particle size was determined by calculating the average of the sizes of more than 300 particles.

2.4. Electrochemical evaluation

Electrochemical measurements were carried out using an Autolab potentiostat (PGSTAT20, Eco Chemie, The Netherlands) in a conventional three-electrode cell with a catalyst coated glassy carbon electrode (working electrode), a Pt coil (counter electrode) and a saturated Ag/AgCl electrode (reference electrode). The glassy carbon substrate was polished with alumina suspension prior to use. To prepare the working electrode, 7 mg catalyst was dispersed ultrasonically in 1 ml diluted Nafion solution (0.05 wt% in ethanol) for 30 min and 10 μl of the suspension was pipetted onto the glassy carbon electrode (d = 5 mm) by a microsyringe and left to dry at room temperature. Prior to the activity measurement, the working electrode was cleaned by CV sweeping in Ar-saturated 0.1 M KOH or 0.5 M H_2SO_4 solution. Then a certain amount (in order to maintain the concentration of the electrolyte) of ethanol was added into the electrolyte to do the activity measurements. The steady state oxidation currents were collected after 15 min of chronoamperometry at each specific potential. All the currents are normalized by the surface area of the glassy carbon substrate and are given in unit of mA cm^{-2}. The impedance spectra were recorded in a constant potential mode with an amplitude of 10 mV and a scanning frequency ranging from 10^4 to 10^{-2} Hz. All electrochemical experiments were conducted at room temperature.

3. Results and discussion

3.1. Physicochemical characterization

XRD patterns of the Pd/C, Rh/C and Pd-Rh/C are shown in Fig. 1. The broad diffraction peak at about 25° is ascribed to the (0 0 2) plane of Vulcan XC-72 carbon. Both Pd/C and Pd–Rh/C show characteristic diffraction peaks of face centered cubic crystalline structure.

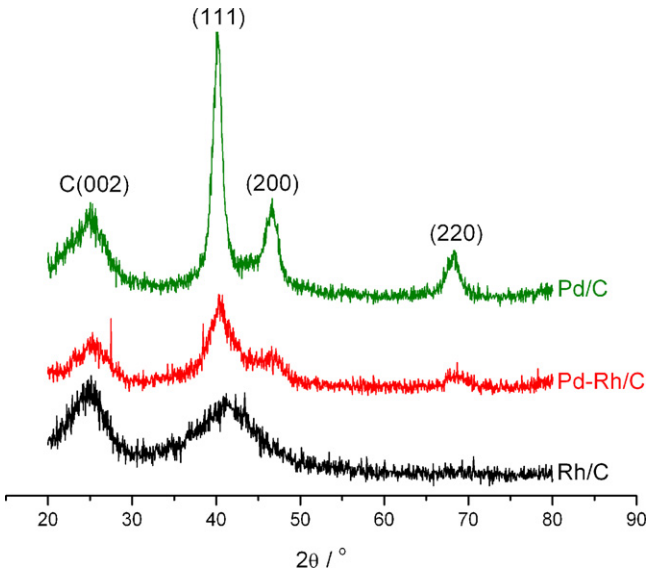

Fig. 1. XRD patterns of the Pd/C, Ph/C and Pd–Rh/C catalysts.

Rh/C, on the other hand, shows only a single diffraction peak (besides the diffraction peak from carbon) at about 41°, indicating that the Rh nanoparticles dispersed on Vulcan XC-72 could be very small or in an amorphous state [15].

Fig. 2 shows the TEM images of the Pd/C, Rh/C and Pd–Rh/C catalysts. Clearly, all the nanoparticles are well dispersed on the carbon surface. The histogram of particle size was obtained by measuring more than 300 nanoparticles at different areas. The average particle sizes of Pd/C, Rh/C and Pd–Rh/C are 4.9 nm, 3.0 nm and 4.2 nm, respectively.

3.2. Catalytic activity of the catalysts in alkaline medium

The cyclic voltammograms of Pd/C, Rh/C and Pd–Rh/C in Ar saturated KOH solution are shown in Fig. 3a. In the forward scan, oxygen adsorption at high potential range can be observed on all the three catalysts. In the backward scan, oxygen desorption occur at low potentials, with Pd/C showing a peak at the highest potential.

The typical voltammograms of ethanol oxidation on Pd/C, Rh/C and Pd–Rh/C are shown in Fig. 3b. In the forward scan, ethanol oxidation starts at low potentials, producing one oxidation peak on both Pd/C and Pd–Rh/C and two oxidation peaks on Rh/C, which is consistent with the literature [16]. Higher oxidation currents at low potentials (i.e., lower than −0.3 V) are observed on Rh/C compared with those on Pd–Rh/C and Pd/C. In the backward scan, the onset of ethanol oxidation occurs at low potentials on all the three catalysts. At high potentials, oxidation of water results in the formation of adsorbed oxygen species (as seen in Fig. 3a), which block the active surfaces [11], leading to negligible oxidation currents. The removal of the oxidized species at low potentials exposes the active surfaces, triggering the large oxidation currents at certain potential points. Consistently, a higher onset potential of ethanol oxidation is observed on Pd/C surface, which results from a higher onset potential of oxygen desorption compared with that on Pd–Rh/C and Rh/C (as seen in Fig. 3a).

Steady state ethanol oxidation currents were measured by chronoamperometry and shown in Fig. 4a–c. The currents collected after polarizing the electrodes at each specific potential for 15 min were plotted against the potential (as shown in Fig. 4d). It can be clearly seen that, at low potentials (i.e., −0.5

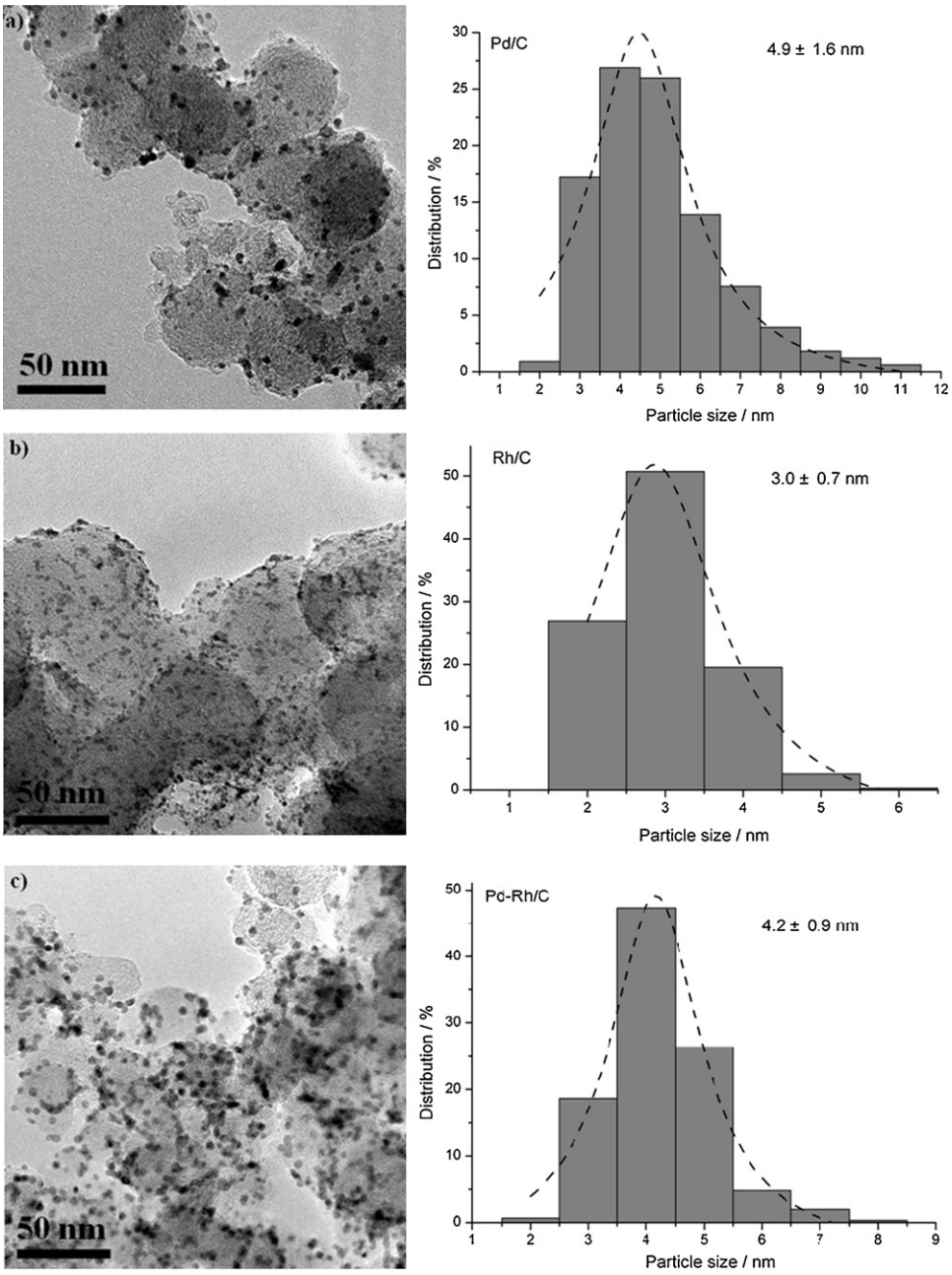

Fig. 2. TEM images of the (a) Pd/C; (b) Rh/C and (c) Pd–Rh/C catalysts.

to −0.3 V), Rh/C shows the largest oxidation currents, indicating a higher catalytic activity of Rh/C for ethanol oxidation compared with Pd/C. At high potentials (i.e., higher than −0.3 V), an obvious current drop on Rh/C is observed, which could be due to the inhibiting effect of the adsorbed oxygen species. On Pd–Rh/C, oxidation current decay is observed only at potentials higher than −0.1 V, indicating that stable inhibiting species (e.g., adsorbed oxygen species) are formed at higher potentials compared with that on Rh/C, which is consistent with our CV results (Fig. 3a).

Fig. 5 shows the complex impedance plots of ethanol oxidation on Pd/C and Rh/C at different potentials. On Pd/C (Fig. 5a), the impedance arcs appear at the first quadrant and the diameter of the arc decreases with the increase of potentials, indicating decreased resistance at higher applied potentials. Different from that on Pd/C, more complicated impedance behaviors are observed on Rh/C (Fig. 5b and c). At low potential range (i.e., −0.5 to −0.3 V), the impedance arcs appear at the first quadrant at high frequency and reverse to the fourth quadrant at low frequency, suggesting pseudo-inductive behavior, which indicates the possible generation of intermediate species during the oxidation process [17]. The different impedance behaviors on Pd/C and Rh/C could be viewed as an indication that ethanol oxidation may follow different reaction pathways on these two catalysts. At −0.25 V and −0.2 V, the impedance plots occur in the second quadrant, indicating negative polarization resistance [18], which suggests that the steady state oxidation current decreases with the increase of applied potential, consistent with our chronoamperometry results (Fig. 4d). At −0.15 V and −0.1 V, large impedance arcs are observed with some instability at low frequency. This is because, as the data presented in Fig. 4 suggests, at high potential (e.g., −0.1 V), ethanol oxidation current is extremely low.

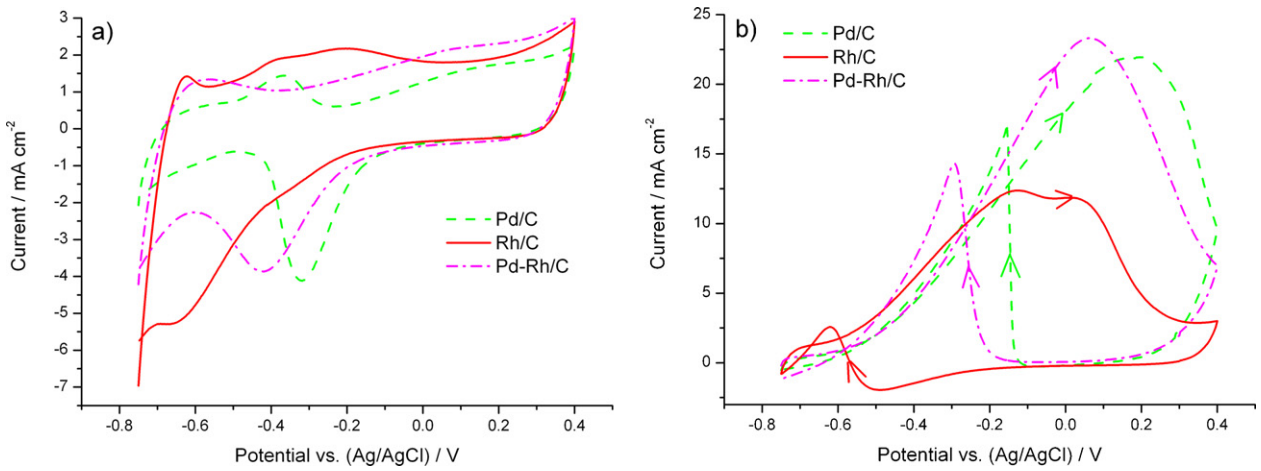

Fig. 3. (a) Cyclic voltammograms of Pd/C, Rh/C and Pd–Rh/C in Ar saturated 0.1 M KOH solution at room temperature with a scan rate of 50 mV s^{-1}; (b) cyclic voltammograms of Pd/C, Rh/C and Pd–Rh/C in Ar saturated 0.1 M KOH + 0.5 M ethanol solution at room temperature with a scan rate of 50 mV s^{-1}.

3.3. Catalytic activity of Pd/C and Rh/C in an acidic medium

The catalytic activities of Pd/C and Rh/C for ethanol oxidation in an acidic medium were evaluated, as shown in Fig. 6. Both Pd/C and Rh/C show no activity for ethanol oxidation in the acidic medium. As discussed by other researchers [7], the difficulty of dehydrogenation of ethanol results in nearly no ethanol oxidation on Pd in acidic mediums. The same explanation is applicable

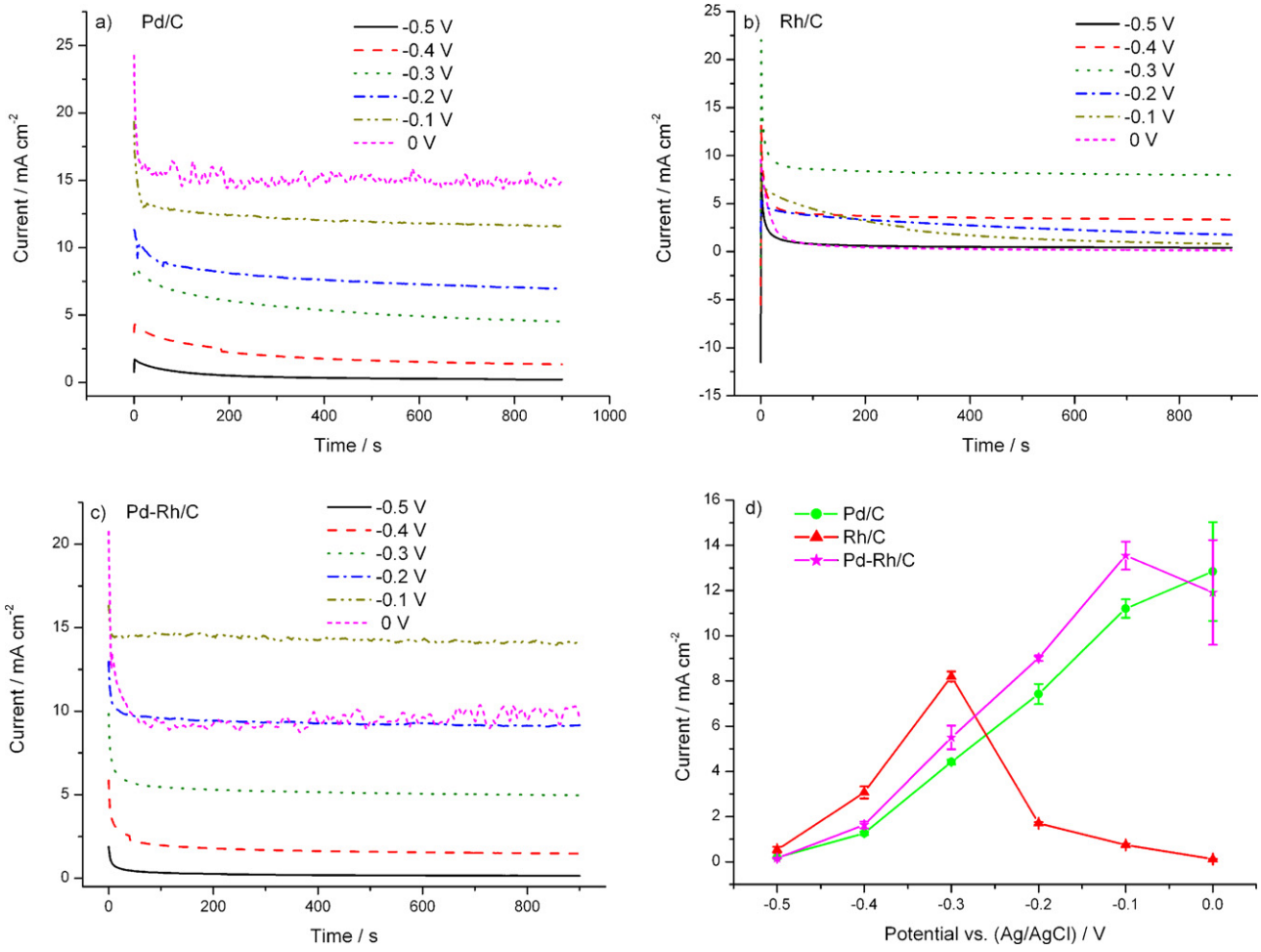

Fig. 4. Chronoamperometry measurements of ethanol oxidation on (a) Pd/C, (b) Rh/C and (c) Pd–Rh/C at different applied potentials in Ar saturated 0.1 M KOH + 0.5 M ethanol solution at room temperature; (d) steady state ethanol oxidation current (averaged by two measurements) after polarizing the electrode at each specific potential in Ar saturated 0.1 M KOH + 0.5 M ethanol solution for 15 min at room temperature.

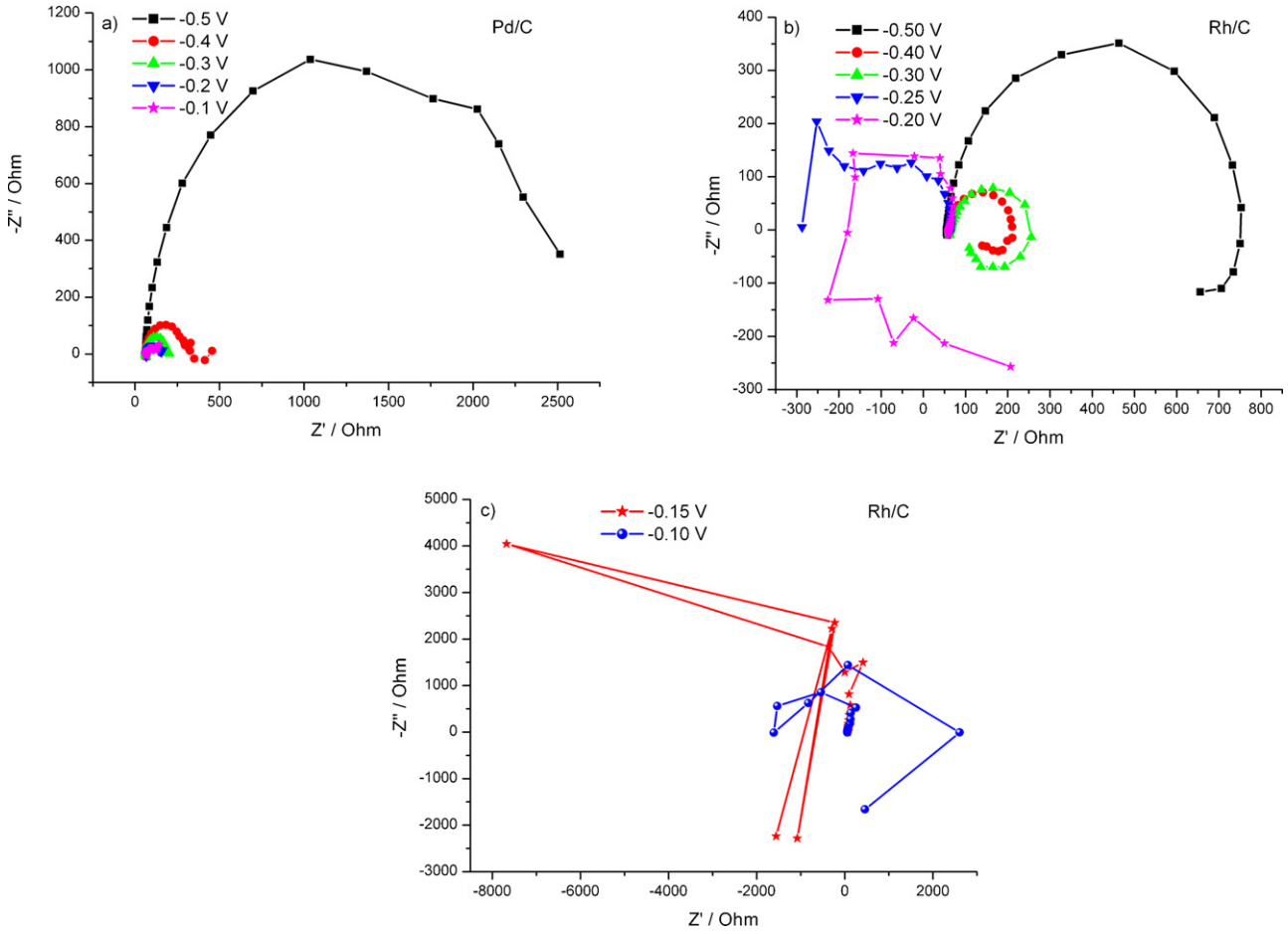

Fig. 5. Complex impedance plots of 0.5 M ethanol oxidation on (a) Pd/C; (b) Rh/C at low potential range and (c) Rh/C at high potential range in Ar saturated 0.1 M KOH solution.

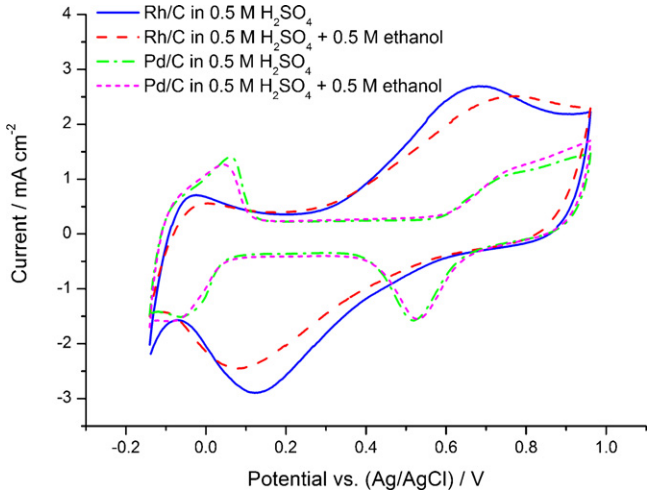

Fig. 6. Cyclic voltammograms of Pd/C, Rh/C in Ar saturated 0.5 M H_2SO_4 solution (with and without 0.5 M ethanol) at room temperature with a scan rate of 50 mV s^{-1}.

here for the zero activity of Rh/C for ethanol oxidation in the acidic medium.

4. Conclusions

Rh/C and Pd–Rh/C nanocatalysts have been synthesized using ethylene glycol and sodium citrate as the reducing and protective reagents. In an alkaline medium, Rh/C shows a higher activity for ethanol oxidation at low potentials compared with Pd–Rh/C and Pd/C. Different impedance behaviors of ethanol oxidation on Pd/C and Rh/C indicate that different ethanol oxidation reaction mechanisms may exist on these two catalysts. This study demonstrated that Rh-based catalysts are promising catalyst candidates for ethanol oxidation in alkaline mediums.

Acknowledgements

The authors gratefully acknowledge the Research Grants Council of the Hong Kong SAR Government for the funding support. Yange Suo thanks the postgraduate scholarship support from the Nanoscience and Nanotechnology program of School of Engineering at HKUST. Technical support on surface analysis from the staff of Materials Characterization and Preparation Facility (MCPF) of HKUST is also appreciated.

References

[1] A.S. Aricò, P. Cretì, P.L. Antonucci, V. Antonucci, Electrochem. Solid-State Lett. 1 (1998) 66–68.
[2] E. Antolini, J. Power Sources 170 (2007) 1–12.
[3] A. Kowal, M. Li, M. Shao, K. Sasaki, M.B. Vukmirovic, J. Zhang, N.S. Marinkovic, P. Liu, A.I. Frenkel, R.R. Adzic, Nat. Mater. 8 (2009) 325–330.
[4] S.C.S. Lai, M.T.M. Koper, Phys. Chem. Chem. Phys. 11 (2009) 10446–10456.
[5] S. Lu, J. Pan, A. Huang, L. Zhuang, J. Lu, Proc. Natl. Acad. Sci. USA 105 (2008) 20611–20614.
[6] J.B. Xu, T.S. Zhao, S.Y. Shen, Y.S. Li, Int. J. Hydrogen Energy 35 (2010) 6490–6500.

[7] G. Cui, S. Song, P.K. Shen, A. Kowal, C. Bianchini, J. Phys. Chem. C 113 (2009) 15639–15642.
[8] C. Xu, L. Cheng, P. Shen, Y. Liu, Electrochem. Commun. 9 (2007) 997–1001.
[9] F. Ksar, L. Ramos, B. Keita, L. Nadjo, P. Beaunier, H. Remita, Chem. Mater. 21 (2009) 3677–3683.
[10] L.-S. Jou, J.-K. Chang, T.-J. Twhang, I.-W. Sun, J. Electrochem. Soc. 156 (2009) D193–D197.
[11] Z.X. Liang, T.S. Zhao, J.B. Xu, L.D. Zhu, Electrochim. Acta 54 (2009) 2203–2208.
[12] X. Fang, L. Wang, P.K. Shen, G. Cui, C. Bianchini, J. Power Sources 195 (2010) 1375–1378.
[13] J.P.I. de Souza, S.L. Queiroz, K. Bergamaski, E.R. Gonzalez, F.C. Nart, J. Phys. Chem. B 106 (2002) 9825–9830.
[14] Y. Suo, I-M. Hsing, Electrochim. Acta 56 (2011) 2174–2183.
[15] Y. Sun, L. Zhuang, J. Lu, X. Hong, P. Liu, J. Am. Chem. Soc. 129 (2007) 15465–15467.
[16] Q. He, S. Mukerjee, B. Shyam, D. Ramaker, S. Parres-Esclapez, M.J. Illán-Gómez, A. Bueno-López, J. Power Sources 193 (2009) 408–415.
[17] I-M. Hsing, X. Wang, Y.-J. Leng, J. Electrochem. Soc. 149 (2002) A615–A621.
[18] Y. Suo, I-M. Hsing, Electrochim. Acta 55 (2009) 210–217.